Laser-Cooled Mercury Ion Frequency Standard *

D.J. Berkeland, J.D. Miller†, J.C. Bergquist, W.M. Itano, and D.J. Wineland
National Institute of Standards and Technology, 325 Broadway, Boulder, CO 80303

Abstract: A stable and accurate frequency standard based on the 40.5 GHz ground-state hyperfine transition in $^{199}Hg^{+}$ ions is described. The ions are confined in a cryogenic linear Paul (rf) trap and laser-cooled to form a linear crystal. With seven ions and a Ramsey interrogation time of 100 s, the fractional frequency stability is $3.3\ (2) \times 10^{-13}\ \tau^{-1/2}$ for measurement times $\tau < 2$ h. The ground-state hyperfine interval is measured to be 40 507 347 996.841 59 (14) (41) Hz, where the first number in parentheses is the uncertainty due to statistical and systematic effects, and the second is the uncertainty in the frequency of the time scale to which our standard is compared.

Atomic frequency standards [1, 2] play vital roles in physics, such as defining the unit of time and other basic units, realizing fundamental constants, and testing basic physical phenomena [3]. A good frequency standard requires that the uncertainty of all systematic effects be small, and that a high measurement precision can be reached in a practical time. Here, we describe a frequency standard based on a laser-cooled linear crystal of $^{199}Hg^{+}$ ions confined in a linear Paul (rf) trap, which satisfies these requirements. The uncertainty from systematic effects (3.4 parts in 10^{15}) is approximately equal to the best values reported, from a cesium beam clock (5 parts in 10^{15}) [4], and a cesium fountain clock (2 parts in 10^{15}) [5], and can be significantly reduced in future experiments.

An important systematic effect for high-resolution spectroscopy and atomic clocks is the second-order Doppler (time-dilation) shift caused by atomic motion. Laser cooling can reduce this shift and has been applied to accurate atomic clocks based on hyperfine transitions in trapped $^{9}Be^{+}$ ions [6] and Cs atoms in a fountain clock [5]. Unfortunately, for trapped ions, part of the atomic motion is due to the trap's electromagnetic field and is not directly affected by laser cooling. In the linear Paul trap [7], driven motion (termed "micromotion") can be significantly reduced by confining the ions near the nodal line of the rf electric field. A limiting case is a linear crystal of ions confined along the field nodal line. For example, if Hg^{+} ions are laser-cooled to the Doppler limit, the magnitude of the time-dilation shift is 2×10^{-18} [8].

Fluctuations in frequency measurements are typically expressed by the two-sample Allan variance [9]

$$\sigma_y^2(\tau) \equiv \frac{1}{2(K-1)} \sum_{k=1}^{K-1} \frac{\left(\langle \omega_k \rangle_\tau - \langle \omega_{k+1} \rangle_\tau \right)^2}{\omega_0^2} \ , \qquad (1)$$

where ω_0 is the angular frequency, and $<\omega_k>_\tau$ is the kth measurement of frequency averaged over time τ. The quantity $\sigma_y(\tau)$ is usually called the frequency stability. If measurement of the atomic states is limited by quantum noise [10], the frequency stability is given by [11]

$$\sigma_y(\tau) = \frac{1}{\omega_0 \sqrt{N\ T_R}} \tau^{-1/2} \ . \qquad (2)$$

In this expression, we assume the atomic transition is driven using Ramsey's method of separated fields [12] with time T_R between applications of radiation pulses, ω_0 is the angular frequency of the atomic transition, and N is the number of atoms (assumed constant). Atoms or ions that have a relatively large hyperfine frequency are particularly attractive since good frequency stability is possible even for small N. Cigar-shaped clouds of ions whose long axes coincide with the nodal line of a linear Paul trap have been employed to realize very stable ($\sigma_y(\tau) \cong 5 \times 10^{-14}\ \tau^{-1/2}$) $^{199}Hg^+$ [13] and $^{171}Yb^+$ [14] microwave clocks using approximately 10^6 ions cooled by a buffer gas. However, the fractional systematic frequency uncertainty in these clocks from the second-order Doppler shift is about 4×10^{-14} [15]. The standard described here demonstrates both good frequency stability and accuracy by using laser-cooled ions that are all confined to the field nodal line.

Figure 1 shows a partial energy level diagram of $^{199}Hg^+$. A small magnetic field ($1\text{-}5 \times 10^{-7}$ T) is applied to break the degeneracy of the $F = 1$ states, isolating the $^2S_{1/2}$ ($F = 0$, $m_F = 0$) $\rightarrow$ (1, 0) hyperfine clock transition ($\omega_0 \cong 2\pi \cdot 40.5$ GHz). Measurements of the Doppler-broadened width of the 282 nm electric quadrupole transition give the temperature of the ions and their heating rate in the absence of laser cooling. Two collinear beams of sum-frequency-generated 194 nm light [16] drive the indicated electric dipole transitions, which are used to cool the ions. For Doppler cooling, the frequency of a primary 194 nm beam p is tuned slightly below that of transition p. Although this is nearly a cycling transition, beam p can off-resonantly excite the ions into the $^2P_{1/2}$, $F = 1$ level, from which they can decay into the $^2S_{1/2}$, $F = 0$ level. To maintain fluorescence, the frequency of a weaker repumping 194 nm beam r is nearly resonant with that of transition r.

For any constant laser polarization and at zero magnetic field, two orthogonal superpositions of the three $^2S_{1/2}$, $F = 1$ magnetic sublevels are dark states. After scattering a few photons, an ion is optically pumped into these states, which scatter no photons. To constantly pump the ions out of the dark states, the 194 nm field must couple each magnetic sub-level of the $^2S_{1/2}$, $F = 1$ state to the $^2P_{1/2}$, $F = 0$ state with a different time dependence. These conditions require that two laser beams, which are tuned to transition p and are not collinear, interact with the ions. The polarizations of the laser beams must be varied to modulate independently at least two of the three level couplings. To maximize the fluorescence rate, the modulation rates should be comparable to the maximum of the three Rabi frequencies. A beam splitter divides the beam comprising beams r and p into two beams, the first of which passes beams through a photo-elastic modulator (PEM), then intersects with the second beam at a relative angle of 40º at the site of the ions. The PEM continuously modulates the polarization of the first beam between right and left circular, while the linear polarization of the second beam remains fixed in the plane formed by the two intersecting beams.

The ions are stored in the linear Paul trap depicted in Fig. 2 [17]. To confine the ions radially, we apply a potential $V \cong V_0 \cos \Omega t$ to two diagonally opposite rods while holding the remaining two rods at ground potential. Typically, $V_0 \cong 150$ V and $\Omega \cong 2\pi \cdot 8.5$ MHz, giving a radial secular frequency $\omega_r = 2\pi \cdot 230$ kHz. A potential $U_0 \cong +10$ V is applied to the two cylindrical endcaps to confine the ions axially in an electrostatic potential characterized by an axial secular frequency $\omega_z \cong 2\pi \cdot 15$ kHz. The ions form a linear crystal along the nodal line of the rf electric field at the axial center of the trap. The trap is placed in an enclosure whose top is also the bottom of a liquid helium Dewar [17]. The cryogenic environment eliminates ion loss and suppresses frequency shifts caused by collisions with background gas.

To reduce Doppler and Stark shifts induced by the trap's rf electric field, we detect and minimize ion micromotion in three noncoplanar directions [18]. We probe the ions in turn with one of the two laser beams propagating at ±20º relative to the axis of the trap, and a third laser beam propagating perpendicular to the plane of the first two. During this process, a magnetic field is applied so that just one of these beams can excite the ions without pumping them into a dark state. The first-order Doppler shift from the ions' micromotion modulates the fluorescence rate at angular frequency Ω. We eliminate this fluorescence modulation by applying a static electric field that forces the ions to the nodal line of the trap's rf electric field and to the axial center of the trap.

We use the Ramsey technique of separated oscillatory fields to probe the clock transition [12]. First, the ions are cooled with both beams *p* and *r* for approximately 300 ms. Next, beam *r* is blocked for about 60 ms to optically pump the ions into the $^2S_{1/2}$, $F = 0$ level. Both beams are then blocked during the Ramsey microwave interrogation period, which consists of two $\pi/2$ microwave pulses of duration $t_R = 250$ ms separated by the free precession period T_R, which we vary from 2 to 100 s in separate runs. Transitions to the $F = 1$ state are detected by reapplying only beam *p* until the ion is optically pumped into the $F = 0$ state (≅ 10-20 ms), while we count the number of detected scattered photons (typically about 150 per ion). This process completes one measurement cycle.

We synthesize the microwave frequency from a low-noise quartz oscillator locked to a reference hydrogen maser [19]. To steer the average microwave frequency into resonance with the clock transition, we step the frequency by $+\Delta f$, then $-\Delta f$, about frequency f_M ($\cong \omega_0/(2\pi)$), and complete a measurement cycle after each step. Usually, the stepped frequencies lie near the half-maximum points of the central Ramsey fringe. On successive measurement pairs, we alternate the signs of the frequency steps to avoid any bias from linear drifts in, for example, the signal amplitude. The difference between the number of detected photons for the pair of measurement cycles gives the error signal ε_M. A digital servo adjusts the average frequency according to

$$f_{M+1} = f_0 + g_p \varepsilon_M + g_i \sum_{m=1}^{M} \varepsilon_m , \qquad (3)$$

where f_0 is the initial value of the frequency, and the proportional gain g_p and the integral gain g_i are independent of each other. Typically, the maximum value of *M* for a single run is about 130. The average frequency for each run is calculated after discarding the first four recorded frequencies f_i, to remove initial frequency offsets.

The stability of the steered microwave frequency when $N = 7$ and $T_R = 100$ s is $\sigma_y(\tau) \cong 3.3\ (2) \times 10^{-13}\ \tau^{-1/2}$, for $\tau \leq 2$ h. Consistently, $\sigma_y(\tau)$ is about twice the value expected from Eq. (2), primarily because of laser intensity fluctuations at the site of the ions. The measured frequency stability is comparable to those of the Cs beam standard NIST-7, for which $\sigma_y(\tau) \cong 8 \times 10^{-13}\ \tau^{-1/2}$ [20], and the Cs fountain standard, for which $\sigma_y(\tau) \cong 2 \times 10^{-13}\ \tau^{-1/2}$ [5].

The average frequency for each run is corrected for the systematic effects shown in Table 1. We first correct the average frequency of a run for the quadratic Zeeman shift due to the static magnetic field B_s. From the measured values of g_J [21] and the ^{199}Hg nuclear magnetic moment [22], the fractional shift is $1.219\ 873\ (5)\ 10^{-21}\ \nu_\pm^2$, where $\nu_\pm$ ($\cong 1.4\ 10^{10}\ B_s$, B_s expressed in Teslas) is the frequency separation in hertz of the $^2S_{1/2}$ ($(0, 0) \rightarrow (1, \pm 1)$) field dependent transitions from the clock transition. The peak-to-peak variation in the static magnetic field between the beginning and end of a run is at most 1×10^{-8} T. Since $B_s \cong 3 \times 10^{-7}$ T, an upper

bound on the uncertainty in this Zeeman shift is 1.4×10^{-15}. We observe no sidebands on the $\Delta m_F = \pm 1$ hyperfine transitions from power line-induced 60 Hz fluctuations in the magnetic field. The corresponding upper limit on the Zeeman shift is $< 2 \times 10^{-20}$ when the static field is 3×10^{-7} T.

We also correct for an ac Zeeman shift that depends linearly on the rf power P_{rf} delivered to the trap. The uncertainty in this correction dominates the overall systematic uncertainty of the clock frequency. This shift can be caused by magnetic fields due to currents at frequency Ω in the trap electrodes that are asymmetric with respect to the trap nodal line. (In an ideal trap, these asymmetric currents are absent.) Allowing for this asymmetry to vary for different ion crystals, we measure the average transition frequency for P_{rf} ranging from about 17 mW ($V_0 \cong 140$ V) to 68 mW ($V_0 \cong 270$ V) for each ion crystal. A fit to these data gives the frequency shift $(d\omega/dP_{rf})/\omega_0$ and the extrapolated frequency at zero rf power ω_0, for that ion crystal. Typically, $(d\omega/dP_{rf})/\omega_0 \cong (2.5 \pm 2.1) \times 10^{-16}$ /mW (within the error, this value is the same for each ion crystal), and the uncertainty in the extrapolated frequency averaged over five ion crystals used in the frequency measurement is 3.2×10^{-15}. The additional uncertainty due to possible rf power measurement inaccuracies is about 3×10^{-16}.

The ac Stark shift due to blackbody radiation at 300 K is 1.0×10^{-16} [23], but should be much less in the cryogenic environment. From the measured 194 nm intensity at the site of the ions when the 194 nm sources are blocked, the ac Stark shift due to stray 194 nm light present during the Ramsey interrogation time is $< 3 \times 10^{-16}$. Because the ion micromotion is minimized, the velocity v of the ion motion and the electric field E_{rf} that the ions experience can be determined from the measured secular temperature [18]. We find that after the 194 nm beams have been off for 100 s, the secular temperature T is less than 25 mK. The corresponding electric field causes a shift of magnitude $< 2 \times 10^{-18}$. This temperature also corresponds to a fractional second-order Doppler shift of magnitude $\leq 3 \times 10^{-17}$.

We search for an added sloping background signal which would shift the measured value of ω_0, by increasing Δf to 4.25 Δf_R when $T_R = 10$ s, and 10.25 Δf_R when $T_R = 25$ s, where Δf_R is the frequency separation between Ramsey fringes. The extrapolated fractional frequency shift is $< 2 \times 10^{-19}$ when locking to the central fringe ($\Delta f = 0.25\ \Delta f_R$) and $T_R = 100$ s. To estimate the effects of the neighboring field-dependent hyperfine transitions, we assume the microwave field coupling strength of the (0, 0) $\rightarrow$ (1, 1) transition equals that of the (0, 0) $\rightarrow$ (1, 0) transition, while the coupling strength of the (0, 0) $\rightarrow$ (1, -1) transition is zero. The corresponding shift is dominated by the ac Zeeman shift, and is less than 1×10^{-17} when $T_R = 100$ s and $B_s = 3 \times 10^{-7}$ T. Frequency shifts due to the phase chirp of the microwaves as they are switched on and off (combined with a possible leakage microwave field present during the free precession time T_R), and to asymmetries in the microwave spectrum scale as $1/T_R$. By varying T_R, we measure the frequency shift from these combined effects to be $-3\ (3) \times 10^{-14}\ /T_R$.

At 4 K, the partial pressure of most gasses is negligible [24], with the possible exception of helium. An upper limit on the collision rate with helium background gas can be inferred from the ions' temperature after the cooling beams have been off for 100 s, where we assume that any heating is caused by collisions with helium atoms. We further assume that the helium collision rate for heating is the same as that which causes frequency shifts; we approximate these rates as the helium density n_{He} times the Langevin rate [25]. Using Cutler's measurement of the helium pressure shift for Hg^+ [26], we can estimate a maximum shift of $< 1 \times 10^{-19}$.

The fits to the transition frequencies as a function of rf power give the extrapolated frequency ω_0 at zero rf power. This value is reproducible over 18 days, which includes 42 runs made over seven days using five different ion crystals. The normalized χ^2 for the measurements of ω_0 from these five ion crystals is 0.77. If we assume that the frequency depends linearly on time, a fit to the data gives a drift of -5 (9) $\times 10^{-16}$/day, consistent with zero.

The hydrogen maser frequency is referenced to primary frequency standards through International Atomic Time (TAI) [3] to obtain the average value $\omega_0 = 2\pi \cdot$ 40 507 347 996.841 59 (13) (5) (41) Hz. The first uncertainty is due to the statistical uncertainty in the extrapolation to zero rf power, and the second to the other systematic shifts shown in Table 1 combined in quadrature. The third, due to the frequency comparisons, is dominated by the published uncertainty in the frequency of TAI [27]. This value of ω_0 is to be compared with the previous most accurate measurement, which gave $\omega_0 = 2\pi \cdot 40\ 507\ 347\ 996.9\ (3)$ Hz [28].

In summary, we have demonstrated a frequency standard based on crystals of laser-cooled $^{199}Hg^+$ ions confined in a linear Paul trap. For T_R = 100 s and N = 7, the fractional frequency stability is $\sigma_y(\tau) \cong 3.3\ (2) \times 10^{-13}\ \tau^{-1/2}$ for $\tau \leq 2$ h. We have measured the clock transition frequency with a fractional systematic uncertainty of 3.4×10^{-15}. This uncertainty is primarily limited by the uncertainty in the Zeeman shift due to fields at the trap frequency Ω. It can be reduced with more measurements of ω_0, and by decreasing Ω and the trap dimensions. Better magnetic shielding will reduce fluctuations in the static magnetic field, and use of a smaller, more tightly confining trap will allow linear crystals with more ions. By monitoring each ion individually, we can determine their internal states with negligible uncertainty, which will eliminate noise due to laser frequency and intensity fluctuations. Finally, we are also investigating the use of entangled states to reduce $\sigma_y(\tau)$ [29].

This work was funded by ONR and ARO. We are grateful to R. Drullinger, S. Jefferts, D. Lee, T. Parker, and F. Walls for useful discussions. We thank F. Walls for providing the microwave frequency synthesizer [19], and T. Parker for frequency comparisons to TAI. We thank P. Huang, D. Lee, M. Lombardi, D. Sullivan, and M. Young for carefully reading this manuscript.

Table 1: Systematic shifts of the clock transition frequency, expressed fractionally. The magnitudes are calculated using P_{rf} = 20 mW, T_R = 100 s, $B_s = 3 \times 10^{-7}$ T and $T_{ambient}$ = 300 K. Here, B_{60} and B_Ω are the magnetic field components at 60 Hz and Ω, I_p is the intensity of beam p during the Ramsey interrogation time, δ_p the detuning of the frequency of beam p from that of transition p, γ the linewidth of the cooling transition, and dS/df the slope of the background added to the Ramsey fringe. Other symbols are defined in the text.

Shift	Scaling	Magnitude of Effect	Overall Uncertainty in Effect
Quadratic Zeeman (static)	$+ \langle B_s^2 \rangle$	2×10^{-14}	1.4×10^{-15}
Quadratic Zeeman (60 Hz)	$+ \langle B_{60}^2 \rangle$	$< 2 \times 10^{-20}$	$< 2 \times 10^{-20}$
Quadratic Zeeman (Ω)	$+ \langle B_\Omega^2 \rangle$	5×10^{-15}	3.2×10^{-15}
Blackbody ac Stark	$- T^4_{ambient}$	$< 1.0 \times 10^{-16}$	$< 1.0 \times 10^{-16}$
Blackbody ac Zeeman [23]	$+ T^2_{ambient}$	$< 1.3 \times 10^{-17}$	$< 1.3 \times 10^{-17}$
Light shift from 194 nm	$\frac{I_p \delta_p}{\delta_p^2 + \frac{1}{4}\gamma^2}$	$< 3 \times 10^{-16}$	$< 3 \times 10^{-16}$
ac Stark (from trap fields)	$- \langle E_{rf}^2 \rangle$	$< 2 \times 10^{-18}$	$< 2 \times 10^{-18}$
Second-order Doppler	$- \langle v^2/c^2 \rangle$	$< 3 \times 10^{-17}$	$< 3 \times 10^{-17}$
Background slope	$- (dS/df)/T_R^2$	$< 2 \times 10^{-19}$	$< 2 \times 10^{-19}$
Neighboring transitions	$1/(B\, t_R\, T_R)$	$< 1 \times 10^{-17}$	$< 1 \times 10^{-17}$
Microwave chirp, leakage and spectrum asymmetries	$1/T_R$	3×10^{-16}	8×10^{-16}
Helium pressure shift	$-n_{He}$	$< 1 \times 10^{-19}$	$< 1 \times 10^{-19}$

Figure 1: Partial energy level diagram of $^{199}Hg^{+}$ in zero magnetic field.

Figure 2: Schematic diagram of the linear trap. The trap is formed by four parallel rods of radius r = 0.38 mm, and two endcaps 4 mm apart. A string of ions is depicted at the trap center.

References

* Work of U.S. Government, not subject to U.S. copyright

† Present address: KLA, Austin, TX

1 Proc. 5th Symp. Freq. Standards and Metrology, ed. J.C. Bergquist, (World Scientific, 1996).

2 P.T.H. Fisk, Rep. Prog. Phys. **60**, 761 (1997).

3 Proc. IEEE: Special Issue on Time and Freq. **79** (1991).

4 R.E. Drullinger, J.H. Shirley and W.D. Lee, in 28th Ann. PTTI Appl. And Planning Mtg., 255 (1996).

5 E. Simon, P. Laurent, C. Mandache and A. Clairon, in 11th Eur. Freq. And Time Forum Neuchatel, 43 (1997).

6 J.J. Bollinger, J.D. Prestage, W. M. Itano, and D.J. Wineland, Phys. Rev. Lett. **54**, 1000 (1985).

7 J. Drees and W. Paul, Z. Phys. **180**, 340 (1964).

8 D.J. Wineland, J.C. Bergquist, J.J. Bollinger, W.M. Itano, D.J. Heinzen, S.L. Gilbert, C.H. Manney, and M.G. Raizen, IEEE Trans. On Ultrasonics, Ferroelectrics, and Frequency Control **37**, 515 (1990).

9 J.A. Barnes, A.R. Chi, L.S. Cutler, D.J. Healey, D.B. Leeson, T.E. McGunigal, J.A. Mullen, Jr., W.L. Smith, R.L. Sydnor, R.F.C. Vessot, and G.M.R. Winkler, IEEE Trans. Instrum. Meas. **IM-20**, 105 (1971).

10 W.M. Itano, J.C. Bergquist, J.J. Bollinger, J.M. Gilligan, D.J. Heinzen, F.L. Moore, M.G. Raizen, and D.J. Wineland, Phys. Rev. A **47**, 3554 (1993).

11 D.J. Wineland, W.M. Itano, J.C. Bergquist, J.J. Bollinger, F. Diedrich, and S.L. Gilbert, Proc. 4th Symp. Freq. Standards and Metrology, ed. A. Demarchi, 71 (Springer Verlag, Heidelberg, 1989).

12 N.F. Ramsey, *Molecular Beams* (Oxford Univ. Press, London, 1956).

13 R.L. Tjoelker, J.D. Prestage, L. Maleki, in Ref. [1], p. 33.

14 P.T.H. Fisk, M.J. Sellars, M.A. Lawn, C. Coles, in Ref. [1], p. 27.

15 R.L. Tjoelker, J.D. Prestage, G.J. Dick, and L. Maleki, Proc. 1993 IEEE Int. Freq. Control Symp., 132 (1993).

16 D.J. Berkeland, F.C. Cruz and J.C. Bergquist, Appl. Opt. **2006**, 4159 (1997).

17 M.E. Poitzsch, J.C. Bergquist, W.M. Itano, and D.J. Wineland, Rev. Sci. Instrum. **67**, 129 (1996).

18 D.J. Berkeland, J.D. Miller, J.C. Bergquist, W.M. Itano, and D.J. Wineland, (submitted for publication to Phys. Rev. A, Aug. 1997).

19 C.W. Nelson, F.L. Walls, F.G. Ascarrunz, and P.A. Pond, Proc. 1992 IEEE Freq. Control Symp., 64 (1992).

20 W.D. Lee, J.H. Shirley, J.P. Lowe, and R.E. Drullinger, IEEE Trans. Instrum. Meas. **44**, 120 (1995).

21 W.M. Itano, J.C. Bergquist, and D.J. Wineland, J. Opt. Soc. Am. B **2**, 1392 (1985).

22 B. Cagnac, Ann. Phys. (Paris) **6**, 467 (1961).

23 W.M. Itano, L.L. Lewis, and D.J. Wineland, Phys. Rev. A **25**, 1233 (1982).

24 G. Gabrielse, X. Fei, W. Jhe, L.A. Orozco, J. Tan, R.L. Tjoelker, J. Haas, H. Kalinowsky, T.A. Trainor, and W. Kells, Am. Inst. Phys. Conf. Ser. **233**, 549 (1991).

25 J.B. Hasted, *Physics of Atomic Collisions* (American Elsevier, 1972).

26 L.S. Cutler, R.P. Giffard, and M.D. McGuire, Proc. 37th Ann. Symp. Freq. Control, 32 (1983).

27 *Bureau International des Poids et Mesures Circular T* **113**, 4 (1997).

28 L.S. Cutler, R.P. Giffard, and M.D. McGuire, Proc. 13th Ann. PTTI Appl. And Planning Meeting, NASA Conf. Publ. 2220, 563 (1981).

29 J.J. Bollinger, W.M. Itano, D.J. Wineland, and D.J. Heinzen, Phys. Rev. A **54**, R4649 (1996).

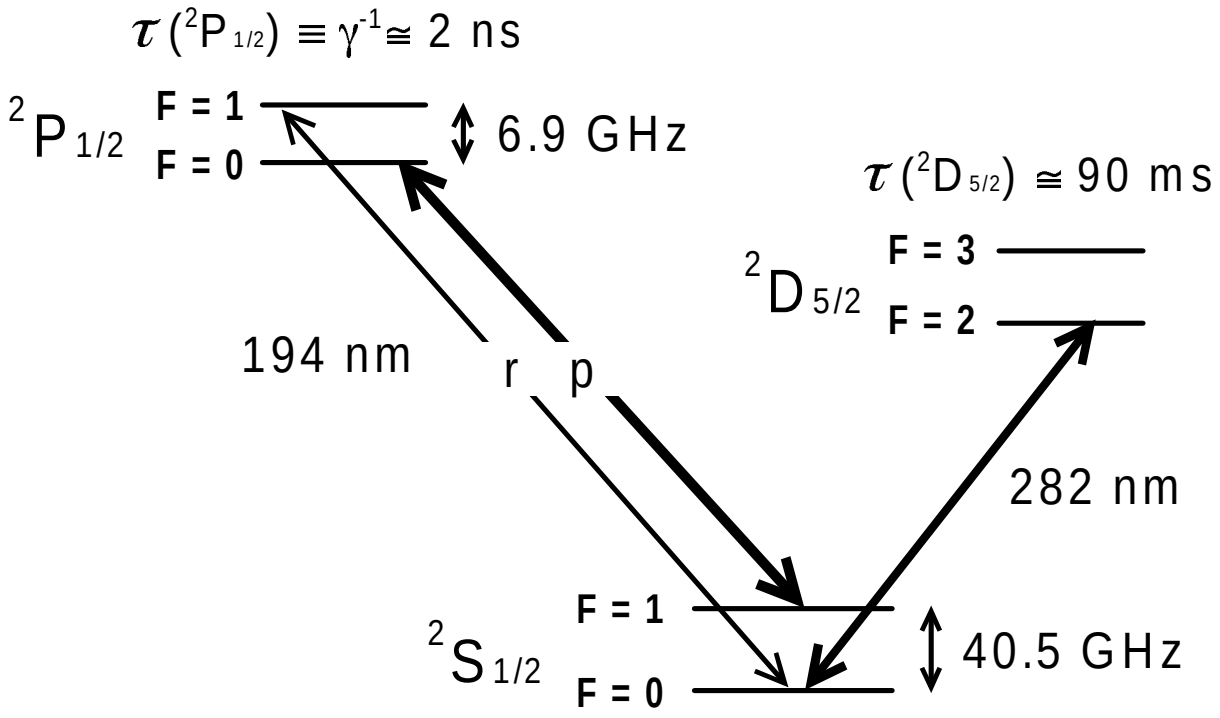
τ(²P1/2) ≡ γ⁻¹ ≅ 2 ns
²P1/2
F = 1
F = 0
6.9 GHz
τ(²D5/2) ≅ 90 ms
²D5/2
F = 3
F = 2
194 nm
r
p
282 nm
²S1/2
F = 1
F = 0
40.5 GHz

Figure 1

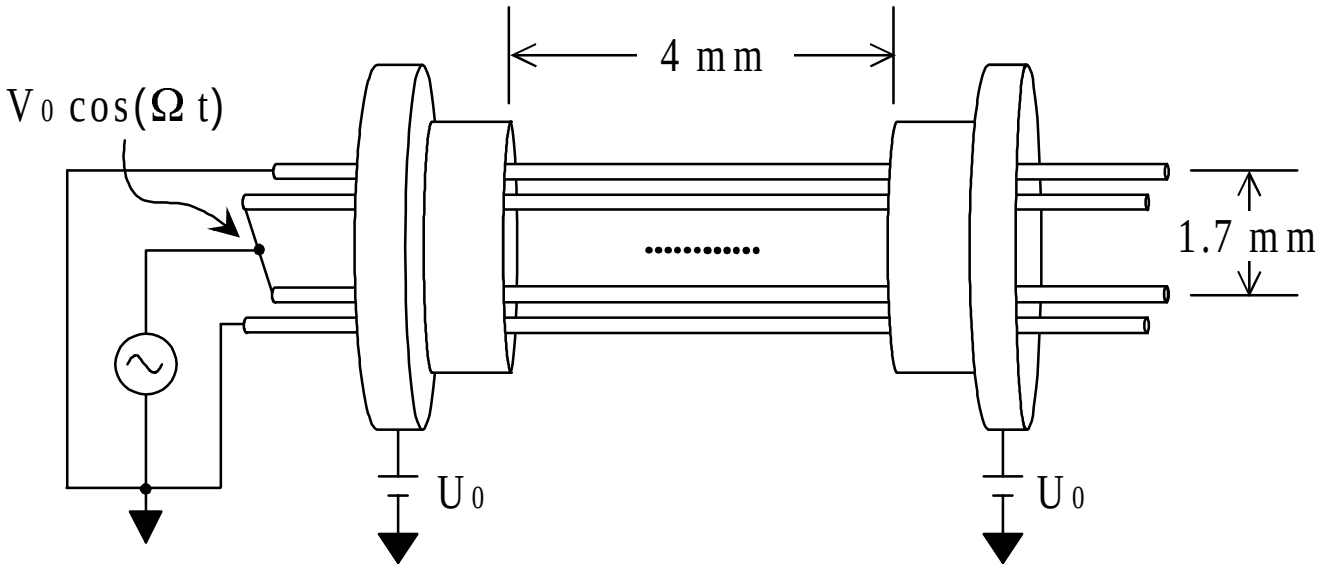

Figure 2